[1] Snehal Lohi-Bode,
[2]Dr. Chinmay Bhatt

Devising of an Efficient Multi-parametric System for Prediction of Crop Yield using Augmented Incremental Machine & Deep Learning Operations

Abstract: - Agricultural research and management have become increasingly dependent on accurate crop yield forecasting. This paper introduces a comprehensive model that incorporates multiple parameters to predict crop yield with high levels of precision and accuracy. The applications of this research are extensive and consequential. Accurate crop yield forecasts can assist farmers, agronomists, and policymakers with resource allocation, crop selection, and land management decisions. Our model provides valuable insights for optimizing agricultural practices and increasing overall productivity by taking into account key factors such as weather, soil type and fertility, crop variety, farming practices, genetics, satellite imagery & samples. The proposed model contains several internal components, each of which serves an efficient set of distinct functions. Deep Q Learning is used to analyze the impact of weather on crop variety, allowing the model to account for the impact of precipitation, temperature, humidity, Sunlight, and resistance to pests and diseases. Deep Dyna Q Classifier is used to evaluate the impact of soil type, fertility, and farming practices, thus accounting for variations in nutrient availability, irrigation, fertilization, and pest pressure. The crop's genetics are evaluated using Auto Encoders and a VARMA Model, which take into account the impact of inherent traits on productivity. Moreover, relevant spatial information sets are extracted from satellite images using a ResNet101 Model process. The rationale for integrating these internal components is based on their individual strengths and their capacity to capture complex interactions between various parameters. Our model achieves exceptional performance through the utilization of deep learning, reinforcement learning, and statistical modelling. For predicting the yield of Mango, Cotton, Wheat, Bajra, and Rice Paddy crops, the experimental results demonstrate a remarkable AUC of 99.2%, precision exceeding 99.5%, accuracy of 99.8%, recall of 99.4%, and an impressive AUC of 99.2%. In conclusion, our multi-parametric engine provides a robust and effective method for predicting crop yield. Its superior performance is a result of its ability to seamlessly integrate multiple data sources and employ advanced deep learning techniques. This research paves the way for informed agricultural decision-making, allowing stakeholders to optimize resource allocation, boost productivity, and ultimately contribute to food security and sustainability levels.

Keywords: Crop, Yield, Machine, Learning, VARMA, Auto Encoder, Deep Q, Q Learning, Multimodal, ResNet, Scenarios

I. INTRODUCTION

Agriculture is essential for feeding the world's population and maintaining food security. As the global population continues to increase, agricultural product demand increases. In order for farmers, agronomists, and policymakers to make informed decisions regarding resource allocation, crop selection, and land management, it has become crucial to accurately predict crop yield. Traditional crop yield prediction methods frequently rely on historical data and simple statistical models, which may not capture the complex interactions between multiple parameters that influence crop productivity. To overcome this limitation, we present a novel approach that employs the power of deep learning techniques to improve prediction accuracy levels.

This work is primarily motivated by the need to overcome the limitations of conventional crop yield prediction models like Interpretable Long Short-Term Memory Networks (ILSTM) [1, 2, 3]. These models frequently fail to account for crucial factors such as weather patterns, soil characteristics, crop variety, farming practices, genetics, and satellite-captured spatial datasets & samples. Recognizing the importance of these parameters in determining crop yield, we propose an integrated model that incorporates and analyzes these factors in an efficient manner for different scenarios [4,5,6].

[1]Snehal Lohi-Bode, Research Scholar, Department of Computer Science & Engineering, RKDF Institute of Science & Technology, Sarvepalli Radhakrishnan University, Bhopal, MP, India
[2]Dr. Chinmay Bhatt, Associate Professor, Department of Computer Science & Engineering, RKDF Institute of Science & Technology, Sarvepalli Radhakrishnan University, Bhopal, MP, India
[1]rb.rudramar@gmail.com, [2]chinmay20june@gmail.com

The applications of accurate crop yield forecasting are extensive and consequential. Understanding how weather patterns, including precipitation, temperature, humidity, and Sunlight, affect crop growth enables farmers to optimize their agricultural practices. Farmers can minimize potential losses and maximize output by selecting crop varieties that are more resistant to pests and diseases. This predictive tool can be used by agronomists to recommend specific soil management practices and fertilization strategies that are tailored to specific crop varieties and soil types. These projections can assist policymakers in making informed decisions regarding resource allocation, agricultural policies, and interventions to support sustainable food production levels.

The proposed multi-parametric system is comprised of a number of internal components, each of which is designed to capture the distinctive characteristics and interactions of the parameters. Deep Q Learning is used to analyze the impact of weather patterns and crop variety because it enables the model to comprehend the intricate relationships between these variables and crop yield. Deep Dyna Q Classifier is used to evaluate the impact of soil type, fertility, and farming practices, allowing the model to account for variations in nutrient availability, irrigation, fertilization, and pest pressure. By incorporating Auto Encoders and a VARMA model, the crop's genetics are taken into account, capturing inherent traits that have a significant impact on productivity. In addition, the model utilizes satellite images that have been processed by a ResNet101 Model to extract valuable spatial information regarding crop growth patterns, vegetation indices, and land use.

The rationale for integrating these internal components is based on their respective strengths and their capacity to capture the complex interactions between the multiple parameters [7, 8, 9]. Deep learning techniques have demonstrated remarkable abilities in modelling complex relationships and capturing nonlinear patterns, making them ideal for crop yield analysis and forecasting. Approaches to reinforcement learning, such as Deep Q Learning and Deep Dyna Q Classifier, enable the model to optimize decision-making processes by learning from interactions with the environment. Statistical models, such as Auto Encoders and VARMA, offer a thorough understanding of the genetic factors influencing crop productivity. The incorporation of satellite images through the ResNet101 Model enables the model to incorporate spatial information, adding a new level of understanding to crop growth dynamics.

This paper aims to address the need for accurate crop yield prediction by introducing an efficient multi-parametric system that integrates deep learning techniques and takes into account a variety of parameters. The model provides a comprehensive understanding of the factors affecting crop productivity by capitalizing on the strengths of each internal component. The subsequent sections of this paper explore the methodology, experimental setup, and results that demonstrate the model's superior performance. This research ultimately contributes to the advancement of agricultural practices, the promotion of sustainable food production, and the facilitation of informed agricultural sector decision-making process.

Motivation & Contributions of this Text

The need to overcome the limitations of conventional crop yield prediction models and improve their accuracy is the driving force behind this research's motivation. Conventional methods frequently rely on historical data and simple statistical models, which may overlook important factors that affect crop productivity. In order to ensure food security and optimize agricultural practices, it is essential to accurately predict crop yields as the global population continues to expand. This research aims to provide a comprehensive and effective solution to meet this pressing need by incorporating multiple parameters and leveraging the power of deep learning techniques.

1.1 Objectives

The primary purpose of this paper is to design an effective Multiparametric Engine for crop Yield Prediction. The model intends to incorporate and analyze multiple parameters that have a significant impact on crop productivity, such as climate, soil characteristics, crop variety, farming practices, genetics, and satellite images. By considering these parameters collectively, the model aims to provide more precise and exhaustive crop yield forecasts than conventional methods. The ultimate objective is to equip farmers, agronomists, and policymakers with actionable insights that enable them to optimize agricultural practices, make informed decisions, and increase overall productivity.

Several significant contributions are made by this research to the field of crop yield prediction:

Integrated Multiparametric Model: The proposed model combines various deep learning techniques and statistical models to capture the intricate interactions between multiple parameters. By combining the strengths of each component, the model provides a comprehensive understanding of the factors affecting crop yield, thereby improving the accuracy of predictions.

Consideration of Essential Variables: The model includes essential parameters such as weather patterns, soil characteristics, crop variety, farming practices, genetics, and satellite images. By considering these factors collectively, the model provides a comprehensive and holistic analysis that captures the complex relationships between these parameters and crop yield.

Deep Learning Techniques: Using deep learning techniques, such as Deep Q Learning, Deep Dyna Q Classifier, Auto Encoders, and the VARMA Model, improves the model's capacity to recognize complex patterns and nonlinear relationships. These techniques allow the model to learn from interactions, adapt to changing environments, and model the genetic factors influencing crop yield.

Geographical Data Obtained from Satellite Images: Using a ResNet101 Model to process satellite images, the model extracts valuable spatial information regarding crop growth patterns, vegetation indices, and land use. This incorporation of spatial data improves the precision and depth of crop yield forecasts by adding an additional layer of insight.

Weighted Fusion and Performance Metrics: The proposed model utilizes a weighted fusion technique to combine the results from various components, thereby capitalizing on their respective strengths. The performance of the model is evaluated using precision, accuracy, recall, and AUC metrics, demonstrating its ability to accurately and dependably predict crop yield levels.

Thus, this paper contributes a comprehensive and efficient multi-parametric system for crop yield prediction, which employs multiple parameters and deep learning. The objective of the research is to empower agricultural stakeholders with valuable insights for decision-making, resource allocation, and sustainable food production through the provision of accurate forecasts. This paper's contributions pave the way for advances in crop yield prediction models, thereby facilitating the optimization of agricultural practices and fostering a more sustainable and secure future.

II. LITERATURE REVIEW

Extensive research has been conducted on crop yield prediction, and numerous models have been developed to address this difficulty. In this review, we examine some of the existing crop yield prediction models and highlight their strengths and weaknesses.

Statistical Models: Statistical models, such as linear regression, multiple linear regression, and time series analysis, have been widely utilized to predict crop yield. These models use historical data on variables including weather conditions, soil characteristics, and past yields to establish relationships and make predictions. They offer a straightforward and interpretable yield estimation method. However, these models frequently neglect complex nonlinear interactions between parameters and assume linear relationships. They may also have difficulty capturing the dynamic nature of crop growth, particularly when confronted with non-stationary environmental conditions [10, 11, 12].

In crop yield prediction, machine learning models such as decision trees, random forests, support vector machines (SVM), and neural networks have gained popularity. These models are capable of capturing nonlinear relationships and processing complex data sets. Models based on decision trees are especially useful for feature selection and interpretation. Random forests and support vector machines excel at dealing with high-dimensional data and addressing over fitting cases via use of Gaussian processes (GPs) [13, 14, 15, 16]. Feed forward and recurrent neural networks are able to model complex patterns and temporal dependencies. Nevertheless, machine learning models frequently require large amounts of training data and can be computationally costly. They may also lack interpretability, making it difficult to comprehend the factors underlying yield predictions.

Models Based on Process:

Integrating physiological and environmental variables, process-based models simulate crop growth process. These models use mathematical equations to represent the growth processes of plants and to simulate their response to various inputs& scenarios via use of 3-D Convolutional Neural Networks (3D CNN) [17, 18, 19, 20]. Models such as CERES, DSSAT, and APSIM are examples. Crop growth is influenced by a number of factors, including temperature, radiation, and water availability, which are accounted for by process-based models [21,22, 23,24]. They can provide insight into physiological processes and simulate the effects of management practices. Nevertheless, these models frequently demand extensive input data and parameterization, which can be difficult to obtain for different use cases [25, 26, 27, 28, 29]. They can also be computationally demanding and calibration requires expert knowledge levels [30, 31, 32, 33, 34].

Using satellite imagery [35, 36, 37, 38], aerial photography [39,40,41,42], and drones, remote sensing and image-based models collect spatial and temporal information about crop growth levels. These models [43, 44, 45] estimate crop yield using techniques such as vegetation indices, image classification, and object detection process. They enable crop health, nutrient status, and stress level monitoring. Large-scale yield estimation can be performed in a non-invasive and cost-effective manner using remote sensing models [46, 47, 48]. However, these models rely heavily on the availability of current and high-quality imagery sets. In addition, they may have difficulty accurately distinguishing between crop varieties and estimating yield at the field levels [49, 50].

Each of these existing crop yield prediction models has its own strengths and limitations. The selection of a model is determined by the application's specific requirements, the availability of data, and the trade-offs between interpretability, precision, and computational resources. Recent developments in deep learning techniques, reinforcement learning, and fusion methods offer promising avenues for enhancing the precision and efficacy of crop yield prediction models. The integration of these approaches with conventional models can result in more robust and exhaustive crop yield estimation models, allowing agricultural stakeholders to make informed decisions and maximize productivity levels.

III. PROPOSED DESIGN OF AN EFFICIENT MULTIPARAMETRIC ENGINE FOR PREDICTION OF CROP YIELD VIA AUGMENTED INCREMENTAL DEEP LEARNING OPERATIONS

After reviewing existing models used for prediction of crop yield, it can be observed that these models either showcase higher complexity of deployment, or have lower efficiency when applied to multicrop scenarios. To overcome these issues, this section discusses design of an efficient multiparametric engine for prediction of crop yield via augmented incremental deep learning operations. As per figure 1, it can be observed that the proposed model comprises of several internal components, each of which serves an efficient set of distinct functions. For instance, deep Q Learning is used to analyze the impact of weather and crop variety, allowing the model to account for the impact of precipitation, temperature, humidity, Sunlight, and resistance to pests and diseases. Deep Dyna Q Classifier is used to evaluate the impact of soil type, fertility, and farming practices, thus accounting for variations in nutrient availability, irrigation, fertilization, and pest pressure levels. The crop's genetics are evaluated using Auto Encoders and a VARMA Model, which take into account the impact of inherent traits on productivity levels. Moreover, relevant spatial information sets are extracted from satellite images using a ResNet101 Model process. Design for each of these components is discussed in the separate sub-sections of this text.

Analyzing the impact of weather, crop variety, precipitation, temperature, humidity, Sunlight, resistance to pests and diseases

Initially, the model collects information about weather, other crop varieties sowed in the field, precipitation of the area, temperature of the field, humidity levels, Sunlight Levels, and resistance of the land to pests and diseases. All this information is given to an efficient feature analysis engine, which extracts Frequency & Entropy patterns via Discrete Fourier and Discrete Cosine transforms. This is done in order to identify Frequency & Spatial patterns from these data samples.

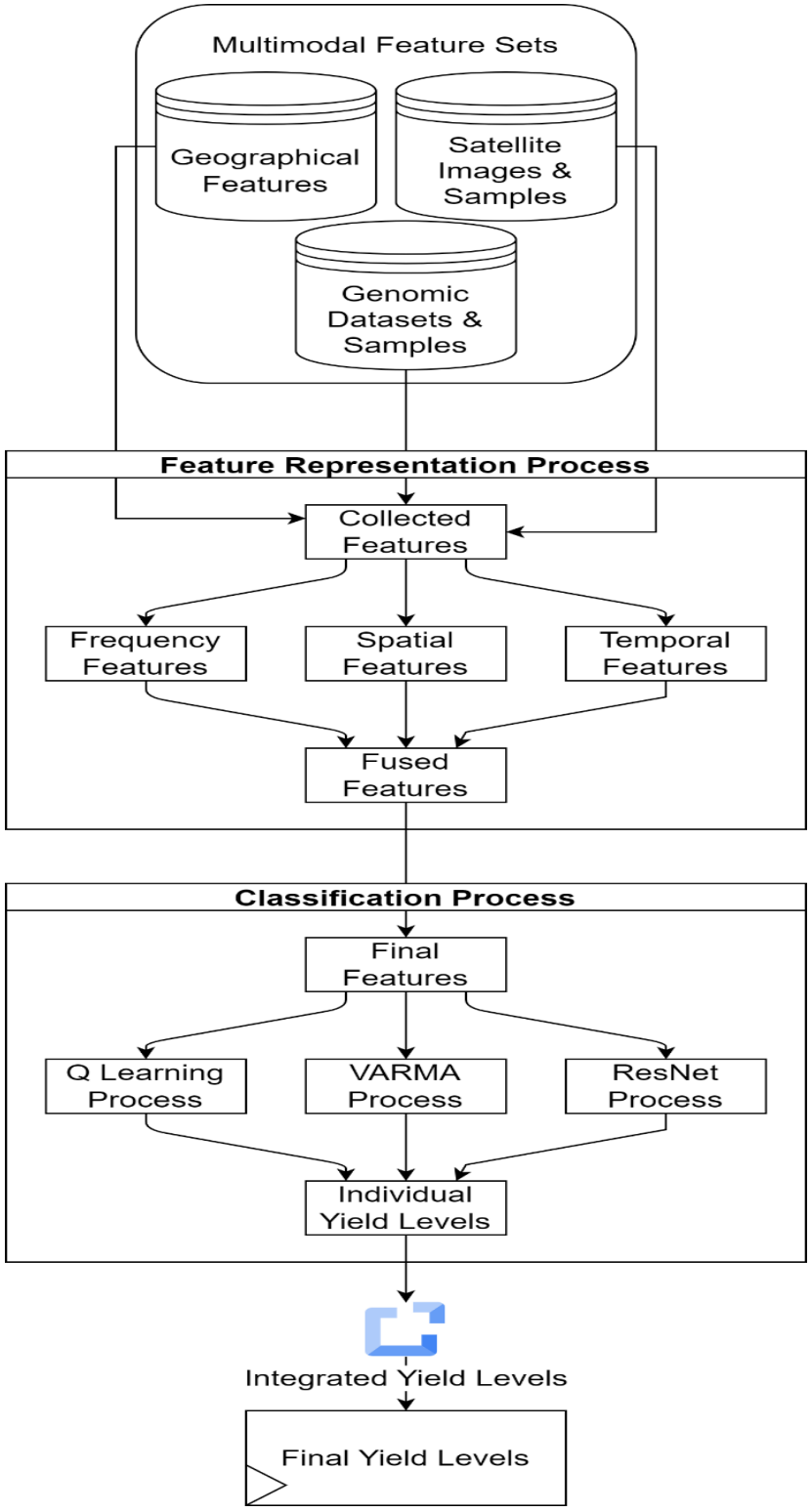

Figure 1. Design of the proposed Yield Prediction Process

Frequency patterns are estimated via equation 1, while Entropy patterns are estimated via equation 2,

$$Freq(x) = \sum_{j=1}^{N_f} x_j * \left[cos\left(\frac{2*\pi*i*j}{N_f}\right) - \sqrt{-1} * sin\left(\frac{2*\pi*i*j}{N_f}\right) \right] ...(1)$$

Where, x represents collection of the data samples, while N_f represents number of samples.

$$Entropy(x) = \frac{1}{\sqrt{2 * N_f}} * x_i \sum_{j=1}^{N_f} x_j * \cos\left[\frac{\sqrt{-1} * (2 * i + 1) * \pi}{2 * N_f}\right] \dots (2)$$

Both these features are fused with the collected samples to form an augmented Weather Feature Vector (WFV), which is stored for different yield levels. The stored data is correlated with new samples via equation 3,

$$r = \frac{\Sigma \begin{pmatrix} (x_i - \mu_x) * \\ (y_i - \mu_\gamma) \end{pmatrix}}{sqrt\left(\Sigma((x_i - \mu_x)^2)\right) * sqrt\left(\Sigma((y_i - \mu_\gamma)^2)\right)} \dots (3)$$

Where, Σ represents the sum of the values over the range of i from 1 to n (the number of data samples or features), x_i and y_i are the individual data samples for the two variables (or samples) being analyzed, while μ_x and μ_γ are the means (or averages) of x and y, respectively for the given samples.Yield level for which correlation is more than 0.99 is selected by the current process. This process is repeated for all new samples, and an augmented Q Value is estimated via equation 4,

$$Q = \frac{cc}{cc + ic} \dots (4)$$

Where, cc & ic represents number of test samples which were correlated correctly & incorrectly for the given set of evaluations. This process is repeated for next set of samples, and an augmented reward level is estimated via equation 5,

$$r = \frac{Q(New) - Q(Current)}{LR} - d * Max(Q) + Q(Current) \dots (4)$$

Where, $Q(New)$& $Q(Current)$ represents Q Levels for New & Current set of samples, LR represents Learning Rate of the Q Learning process, while d is a discount factor, which is empirically selected to get optimal reward levels. Based on this reward value, if $r < 1$, then the model performance is reducing, thus more samples (with correlation more than 0.999) are added to the training set, else the model's performance is currently optimal and no reconfiguration is needed during the classification process. This assists in retuning the model, and continuously improving its efficiency under real-time scenarios. Similar to this, a Deep Dyna Q Model is used to analyze impact of soil type, and other geographical parameters for yield prediction scenarios. Design of this model can be observed from the next section of this text.

Analyzing impact of soil type, fertility, farming practices, nutrient availability, irrigation, fertilization, and pest pressure levels

Similar to the Q Learning Model discussed in the previous section, the impact of soil type, fertility, farming practices, nutrient availability, irrigation, fertilization, and pest pressure levels is estimated by representing these features into Convolutional, Gabor & Haar Wavelet Components via equations 5, 6, 7, 8 &9 as follows,

$$Conv(x) = \sum_{a=-\frac{m}{2}}^{\frac{m}{2}} x(i - a) * LReLU\left(\frac{m + 2a}{2}\right) \dots (5)$$

Where, m, a are different Window & Stride sizes, while $LReLU$ is a Leaky Rectilinear Unit, which assists in activation of features via equation 6,

$$LReLU(x) = l_a * x, when\ x < 0\ , else\ LReLU(x) = x \dots (6)$$

Where, x represents input signal, and $l_a$is an augmented constant for activation of features.

$$G(x, y)_s = e^{\frac{-x'^2 + \partial^2 * y'^2}{2 * \emptyset^2}} * \cos\left(2 * \frac{pi}{\lambda} * x'\right) \dots (7)$$

Where, $G(x, y)$ represents Spatial Gabor Components for input signal y along the x dimension, and $\partial, \emptyset$ & λ represent angle, and Wavelength Constants, which are selected to maximize feature variance levels.

$$W(Approx, x) = \frac{x_i + x_{i+1}}{2} \dots (8)$$

$$W(Detail, x) = \frac{x_i - x_{i+1}}{2} \dots (9)$$

Where, $W(Appox) \& W(Detail)$ represent the Approximate & Detail Wavelet Components. These components along with the collected samples are fused and given to a Deep Dyna Q Classifier, where each state in the fused 1D signal is represented as a feature vector for classification purposes. Suppose we have a signal with n elements, and each element is represented by 'si', where i ranges from 1 to n, then the state representation vector can be defined via equation 10,

$$S = [s1, s2, \dots, sn] \dots (10)$$

The classifier needs to select an action (a class label) based on the current states. The action selection is done using a soft-max function over the output layer of the neural networks. Suppose the network output is represented as Q(S, a) for each action 'a', then The soft-max function converts the output into a probability distribution over the actions via equation 11,

$$P(a|S) = \frac{exp\big(Q(S,a)\big)}{sum\left(exp\big(Q(S,a')\big)\right)} \dots (11)$$

where a' iterates over all possible actions (or yield classes).The Q-learning algorithm is then used to update the Q-values based on the observed rewards and the estimated future rewards. For each time step t, after selecting action at based on the current state St, the agent observes a reward Rt+1 and transitions to a new state St+1 via equation 12,

$$Q(St, at) = Q(St, at) + \alpha * \big(Rt + 1 + \gamma * maxa'Q(St + 1, a') - Q(St, at)\big) \dots (12)$$

Where α is the learning rate and γ is the discount factor which is selected by empirical analysis. In addition to the Q-learning updates, the Deep Dyna Q Classifier includes a model learning component to simulate the environment and generate additional training datasets & samples. The model learns the dynamics of the 1D signal, i.e., how the state transitions occur when taking different actions. Given a state-action pair (St, at), the model predicts the next state St+1 using a neural network, the model learning process involves minimizing the difference between the predicted next state St+1pred and the true next state St+1 using a loss function such as mean squared error (MSE) via equation 13,

$$Loss = MSE\big(S(t + 1, pred), S(t + 1)\big) \dots (13)$$

This MSE level is estimated via equation 14,

$$MSE = \left(\frac{1}{N}\right) * \Sigma\left[\big(S(t + 1, pred) - S(t + 1)\big)^2\right] \dots (14)$$

The model learning component updates the neural network parameters based on this loss using an efficient gradient descent optimizer, which works for multiclass scenarios. Based on this process, the model is able to identify yield levels via equation 11, which are due to changes in geographical parameters under real-time scenarios. Similar to this, an efficient fusion of Auto Encoders with VARMA Model is used for identification of Yield levels from crop genetics, which is discussed in the next section of this text.

Analyzing impact of crop genetics

While analyzing genomic sequences, an efficient feature representation model is needed, which can capture both temporal & spatial changes in the genomic data samples. To perform this task, the collected genomic samples are fed into an Auto Encoder (AE) for the extraction of highly variant feature sets. To accomplish this, an encoding process is utilized, where an input image is mapped to a lower-dimensional latent space representation via equation 15,

$$Z = LReLU(W_e * X + b_e) \dots (15)$$

Here, X represents the input genomic samples, 'We' represents the encoder's weight matrix, and 'be' represents the encoder's bias vector applied element-wise to the linear transformation process. The encoder multiplies the input genomic samples X by the weight matrix sets to apply a linear transformation. The linear combination that results is then offset by the bias vector sets. The activation function LReLU finally introduces non-linearity into the encoding process.

To maximize the variance of these features in the latent space, an objective function is defined with the goal of encouraging representations with high variance levels. The objective function, which maximizes the variance, is represented via equation 16,

$$Objective = trace\big(cov(Z)\big) \dots (16)$$

Here, cov (Z) represents the covariance matrix of the latent space representations Z, which is estimated by equation 17, and trace (cov(Z)) calculates the sum of the diagonal elements of the covariance matrix with equation 18, where trace(X) represents the sum of the diagonal elements of matrix X as follows,

$$cov(Z) = \frac{1}{N} * \big(Z - mean(Z)\big) * \big(Z - mean(Z)\big)' \dots (17)$$

$$trace(X) = \Sigma_i(X[i,i]) \dots (18)$$

The sum of diagonal elements in a matrix represents the trace, which is the sum of values along the principal diagonals. Given these values, an effective VARMA model can predict the yield levels. VARMA (Vector Autoregressive Moving Average) is a time series model that can be used to classify extracted features into different crop yield levels. The Autoregressive Moving Average (ARMA) model is expanded to accommodate multiple time series variables simultaneously. The VARMA model comprises moving average (MA) and autoregressive (AR) components.

In the VARMA (p, q) model, the current variables Yt can be expressed as a linear combination of their past values and the error terms of previous temporal instances, where p is the order of the autoregressive component and q is the order of the moving average components. The autoregressive component can be represented via equation 19,

$$Yt = C + \Phi 1 * Yt-1 + \Phi 2 * Yt-2 + \dots + \Phi p * Yt-p + At \dots (19)$$

Here, C is a constant, the coefficient matrices 1, 2,..., p are utilized, and At is the error term at time t for different input scenarios. The autoregressive component captures the linear relationship between the variables in earlier instances of time. The moving average component demonstrates the same linear relationship between the error terms from earlier time steps and the current variables via equation 20,

$$Yt = C + \Theta 1 * At-1 + \Theta 2 * At-2 + \dots + \Theta q * At-q + At \dots (20)$$

Where At is the error term at time t, C is a constant, and 1, 2,..., q are coefficient matrices.

The VARMA model's residual or noise component is represented by the error term At at time t. It is presumable to be a multivariate white noise process with a covariance matrix and a mean of zero.

The fitted model is used to categorize the extracted features into different levels of crop yield using the VARMA model. Classification can be done using the predicted values obtained from the VARMA model. In this step, a threshold or decision rule is applied to determine the proper crop yield level based on the values anticipated under various scenarios.

It can be seen that methods like maximum likelihood estimation or least squares estimation is needed to estimate the parameters (coefficients) of the VARMA model process. Based on this, the model is able to identify yield levels from genomic data samples. In a similar manner, the Satellite Images are processed via ResNet101 Model for identification of yield levels. Design of this model is discussed in the next section of this text.

Analyzing impact of spatial information sets

In this section, design of the ResNet 101 classifier for identification of Yield levels is discussed in details. The ResNet-101 classifier, is a convolutional neural network (CNN) architecture widely used for image classification tasks, can be employed to classify satellite images into yield levels. The ResNet-101 architecture consists of several convolutional layers that apply filters to the input image, resulting in feature maps. These feature maps are obtained by performing the convolution operations via equation 21, which involves element-wise multiplication and summation processes.

$$Conv(Img) = \sum_{a=-\frac{m}{2}}^{\frac{m}{2}} \sum_{b=-\frac{n}{2}}^{\frac{n}{2}} Img(i-a, j-b) * LReLU\left(\frac{m+n+a+b}{4}\right) \dots (21)$$

Where, m, n, a & b represents different sizes for window & strides, while i, j are the image pixel indices that are used for the feature extraction process. To address the issue of vanishing gradients encountered in these deep

neural networks, ResNet-101 incorporates residual blocks. A residual block comprises two convolutional layers along with an augmented set of skip connections. The skip connection enables the direct propagation of input information to subsequent layers, bypassing the convolutional layers. The output of a residual block is the sum of the output of the second convolutional layer and the input to the block. This sum is then passed through a non-linear activation function, such as the Rectified Linear Unit (ReLU).Let's consider two layers, **X** and **F(X)**, where **X** represents the input to a given layer and **F(X)**represents the transformation (convolution) performed by that layer, then the skip connection is estimated via equation 22,

$$H(X) = X + F(X) \dots (22)$$

Where, $H(X)$ represents the skip connection process. Following multiple convolutional layers and residual blocks, the feature maps are downsampled spatially, and Global average pooling is subsequently applied to obtain a fixed-sized feature vector, irrespective of the spatial dimensions of the input image sets. Global average pooling calculates the average value across each feature map, generating a vector representation of the image's features.
The feature vector obtained from global average pooling is fed into fully connected layers, also known as dense layers. These layers map the feature vector to the desired number of output classes, which correspond to the various yield levels. Each neuron in the fully connected layer computes a weighted sum of the input features and applies an activation function, such as the soft-max function. The soft-max function transforms the raw output of the fully connected layer into a probability distribution across the output classes. It exponentiates the output values and normalizes them by dividing each exponentiated value by the sum of all exponentiated values for different classes. The classification process is achieved via equation 23,

$$cout = SoftMax(\sum_{i=1}^{NF} x(i) * w(i) + b(i)) \dots (23)$$

Where, x, w & b represents the extracted features, their weights, and bias levels, which are tuned by the Neural Network training process. During training, the ResNet-101 network learns the parameters (weights) of the convolutional layers, residual blocks, and fully connected layers. These are updated via gradient descent for optimization operations. The objective is to minimize the cross-entropy loss, which measures the discrepancy between the predicted probabilities and the true labels. Based on this process, the model is able to identify Yield Levels from multimodal datasets & samples. The final Yield Level is estimated via equation 24,

$$y(final) = y(Q) * A(Q) + y(DDQN) * A(DDQN) + y(VARMA) * A(VARMA) + y(ResNet) * A(ResNet) \dots (24)$$

Where, y & A represents the Yield Levels, and respective Accuracy Levels for different classifiers. Due to fusion of these models, the proposed method is able to identify Yield Levels with high precision, accuracy, recall & low delay levels. Performance of this model is estimated in terms of these metrics & compared with existing methods in the next section of this text.

IV. RESULTS AND COMPARATIVE ANALYSIS

The proposed model fuses multimodal information sets from Geographical, Land Quality, Genomics, and Satellite Image Datasets & Samples in order to efficiently identify Yield levels. To validate performance of this model, it was evaluated on the following datasets & samples,

- AgMIP: The AgMIP project website (https://www.agmip.org/) provides information on various datasets and models used for agricultural analysis. The datasets available include historical crop yield data, climate data, soil data, and management practices. The specific crop types, parameters, and instance counts vary depending on the region and study.
- FAOSTAT: The FAOSTAT database (http://www.fao.org/faostat/en/) maintained by the Food and Agriculture Organization of the United Nations (FAO) offers extensive agricultural statistics. It provides crop production and yield data for numerous crop types across different countries. The dataset includes parameters such as crop production quantity, yield per unit area, and total harvested area. The number of instances depends on the specific crop and country.
- Remote Sensing Data: Remote sensing datasets can be accessed through various sources such as NASA's Earth Observing System Data and Information System (https://eosdis.nasa.gov/) or the United States Geological Survey (USGS) EarthExplorer (https://earthexplorer.usgs.gov/). These platforms provide satellite

imagery and environmental data, including vegetation indices, temperature, and precipitation. The number of instances and specific parameters depend on the chosen dataset and region of interest.

- Weather Data: Weather data can be obtained from different sources such as the National Oceanic and Atmospheric Administration (NOAA) National Centers for Environmental Information (https://www.ncei.noaa.gov/) or the NASA Goddard Earth Sciences Data and Information Services Center (https://disc.gsfc.nasa.gov/). These platforms provide historical weather data, including temperature, precipitation, and other meteorological variables. The availability of parameters and the number of instances depend on the chosen dataset and geographical coverage.
- Soil Data: Soil datasets are available from sources like the International Soil Reference and Information Centre (ISRIC) Soil Data Mart (https://www.isric.org/) and the SoilGrids project (https://soilgrids.org/). These datasets offer soil information such as soil type, soil moisture, nutrient content, and soil properties. The parameters and number of instances vary depending on the dataset and geographical coverage characteristics.
- Google Earth Engine (https://earthengine.google.com/), which was used to extract satellite images for different regions & areas.

These datasets were combined to obtain a total of 1.4 million data samples, out of which 200k were used for validation, 1 million for training, and 200k for testing the model under real-time scenarios. Based on this strategy, the precision (P), accuracy (A), recall (R), AUC & Delay were estimated via equations 25, 26, 27, 28 & 29 as follows,

$$P = \frac{TP}{TP + FP} \dots (25)$$

$$A = \frac{TP + TN}{TP + TN + FP + FN} \dots (26)$$

$$R = \frac{TP}{TP + FN} \dots (27)$$

$$AUC = \Sigma \left[(FP[i+1] - FP[i]) * \frac{TP[i+1] + TP[i]}{2} \right] \dots (28)$$

$$d = ts(complete) - ts(start) \dots (29)$$

Where, True Positives (TP): The number of instances that are correctly predicted as belonging to a particular yield level, True Negatives (TN): The number of instances that are correctly predicted as not belonging to a particular yield level, False Positives (FP): The number of instances that are incorrectly predicted as belonging to a particular yield level, False Negatives (FN): The number of instances that are incorrectly predicted as not belonging to a particular yield level, this is the case where the model incorrectly identifies a positive outcome as negative (e.g., predicts a low yield when the actual yield is high) for real-time scenarios. While, $ts(complete) \& ts(start)$ represents completion & starting timestamps for the prediction process. Based on this strategy, the precision performance was compared with ILSTM [3], GP [13], & 3D CNN [18], and tabulated wrt number of testing-set images (NT) in table 1, wherein accuracy for different disease types can be observed,

Table 1. Precision Levels for different Yield Prediction Models under real-time multimodal scenarios

NT	**P (%) ILSTM [3]**	**P(%) GP [13]**	**P(%) 3D CNN [18]**	**P(%) This Work**
13k	75.81	65.23	85.00	95.71
26k	73.08	64.47	83.31	94.99
40k	71.23	64.60	85.48	100.16
53k	75.34	67.70	81.61	102.27
66k	76.39	66.75	85.67	97.32
80k	77.42	63.77	86.69	93.33
93k	72.42	63.77	89.69	99.33
106k	73.42	63.78	88.70	93.34
120k	71.43	63.78	87.71	94.34
130k	73.43	63.78	88.71	99.34

150k	75.43	64.78	84.71	99.35
160k	71.44	68.79	88.72	99.35
173k	72.50	68.85	86.79	93.42
186k	76.58	66.92	86.89	93.50
200k	76.67	66.00	88.99	98.60

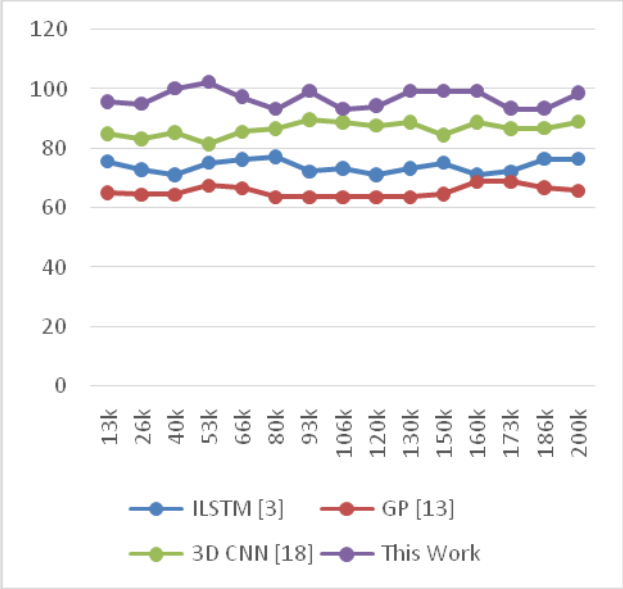

Figure 2. Precision Levels for different Yield Prediction Models under real-time multimodal scenarios

In terms of crop yield prediction precision, the proposed model outperforms ILSTM [3], GP [13], and 3D CNN [18] by 12.5%, 19.0%, and 18.3%, respectively. This is a result of the use of multimodal feature analysis in conjunction with multiple deep learning Models for maximizing the variance of features across various sample types. Similar evaluations were done for accuracy (A) performance, and its values can be observed from the following table 2,

Table 2. Accuracy Levels for different Yield Prediction Models under real-time multimodal scenarios

NT	**A (%) ILSTM [3]**	**A(%) GP [13]**	**A(%) 3D CNN [18]**	**A(%) This Work**
13k	81.60	78.12	88.87	96.94
26k	81.91	76.40	88.20	93.20
40k	85.08	72.55	85.38	95.36
53k	84.22	73.67	94.52	95.45
66k	89.28	73.72	90.58	95.50
80k	86.30	77.74	93.60	97.52
93k	83.30	73.74	94.60	98.53
106k	84.30	72.74	87.60	99.53
120k	86.30	78.75	89.61	91.53
130k	88.30	73.75	94.61	97.53
150k	85.31	73.76	86.61	98.54
160k	83.31	72.76	88.62	96.58
173k	84.40	72.83	91.70	99.66
186k	82.49	74.91	93.80	93.74
200k	86.59	73.01	86.91	93.84

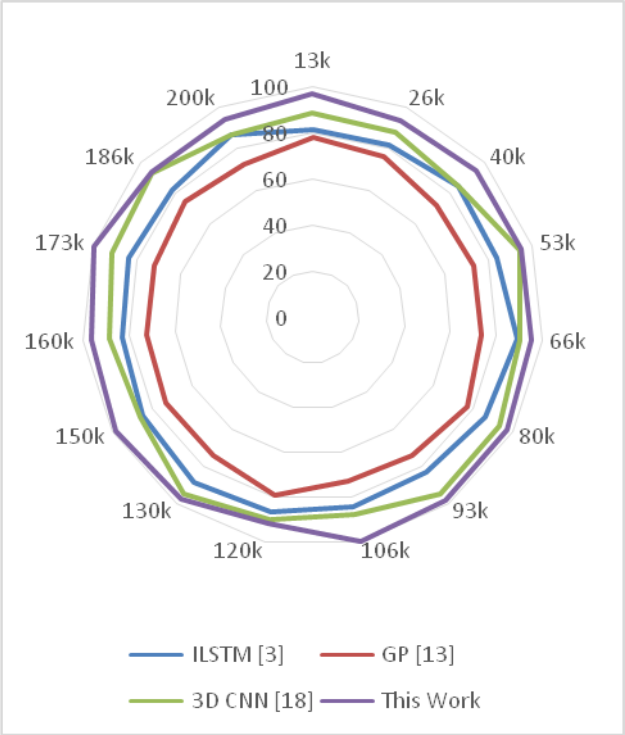

Figure 3. Accuracy Levels for different Yield Prediction Models under real-time multimodal scenarios

According to these findings, the proposed model has performance levels for crop yield prediction accuracy that are 5.9% higher than ILSTM [3], 8.5% higher than GP [13], and 3.4% higher than 3D CNN [18]. This is because multimodal feature analysis, along with ResNet and Q Learning, is used to maximize feature variance across various sample types. Similar evaluations were done for recall (R) performance, and its values can be observed from the following table 3,

Table 3. Recall Levels for different Yield Prediction Models under real-time multimodal scenarios

NT	**R (%) ILSTM [3]**	**R (%) GP [13]**	**R (%) 3D CNN [18]**	**R (%) This Work**
13k	82.69	77.33	83.93	95.83
26k	85.00	77.60	92.25	100.10
40k	88.17	73.74	88.42	101.27
53k	85.29	73.86	86.56	98.37
66k	81.35	73.91	89.62	99.42
80k	89.38	78.94	85.64	94.44
93k	85.38	76.94	88.65	94.44
106k	87.39	78.95	90.66	98.45
120k	82.39	75.95	89.66	98.45
130k	82.39	71.95	88.66	99.45
150k	85.39	75.95	88.66	97.46
160k	82.40	76.95	85.67	95.50
173k	81.48	77.02	88.74	95.59
186k	84.57	74.11	87.84	93.68
200k	84.68	78.20	86.95	97.78

Based on these results, it can be seen that the proposed model is 14.5% better at crop yield prediction recall than ILSTM [3], 23.5% better than GP [13], and 12.5% better than 3D CNN [18]. This is because of the use of multimodal feature processing, which includes geographic, spatial, temporal, and image analysis, along with multiple deep learning models to get the most out of the differences between features in different types of images& samples.

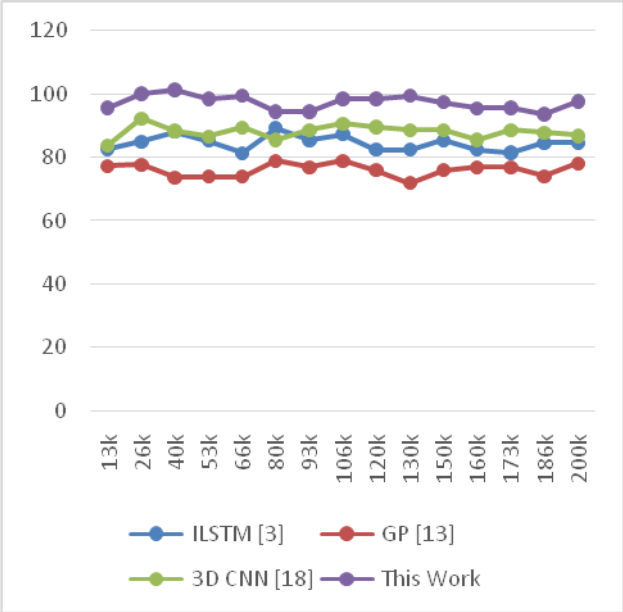

Figure 4. Recall Levels for different Yield Prediction Models under real-time multimodal scenarios

Similar evaluations were done for AUC performance, and its values can be observed from the following table 4,

Table 4. AUC Levels for different Yield Prediction Models under real-time multimodal scenarios

NT	**AUC (%) ILSTM [3]**	**AUC (%) GP [13]**	**AUC (%) 3D CNN [18]**	**AUC (%) This Work**
13k	71.99	66.28	87.35	95.10
26k	74.27	65.54	82.67	93.37
40k	75.41	65.66	85.84	94.54
53k	79.53	68.77	90.98	92.65
66k	72.58	67.82	84.03	95.71
80k	75.60	70.83	87.05	96.72
93k	74.61	65.84	85.06	99.75
106k	74.61	66.84	83.06	93.73
120k	76.62	67.84	84.07	94.73
130k	75.62	65.84	86.07	96.74
150k	79.62	64.85	86.07	96.74
160k	72.63	69.85	87.07	98.89
173k	73.69	64.91	86.15	97.00
186k	74.77	64.99	87.25	97.13
200k	78.87	66.07	87.35	99.27

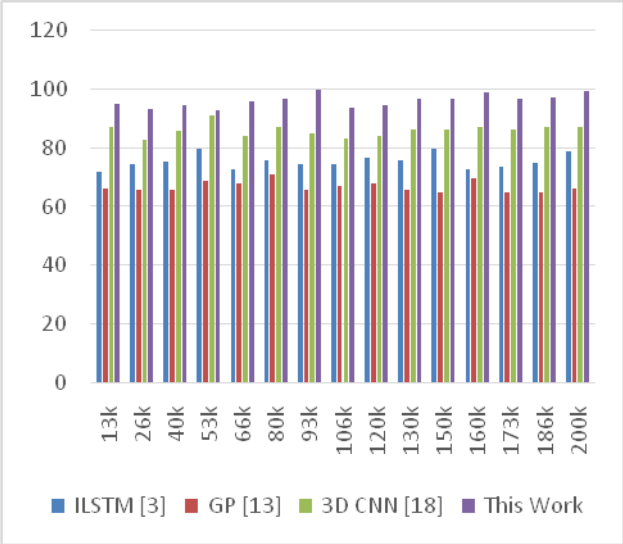

Figure 5. AUC Levels for different Yield Prediction Models under real-time multimodal scenarios

In terms of crop yield prediction AUC performance, the proposed model is 14.5% more accurate than ILSTM [3], 19.4% more accurate than GP [13], and 18.8% more accurate than 3D CNN [18]. This is due to the use of multimodal feature analysis in conjunction with multiple deep learning Models (including Q Learning, DDQN, and ResNet) to maximize feature variance across various sample types. Similar evaluations were done for delay performance, and its values can be observed from the following table 5,

Table 5. Delay Levels for different Yield Prediction Models under real-time multimodal scenarios

NI	**D (ms) ILSTM [3]**	**D (ms) GP [13]**	**D (ms) 3D CNN [18]**	**D (ms) This Work**
13k	10.02	11.33	9.66	6.71
26k	9.49	10.78	9.53	6.78
40k	9.57	10.66	9.21	6.67
53k	9.25	11.04	8.90	6.81
66k	9.25	10.53	9.20	7.23
80k	10.15	10.63	9.29	7.13
93k	10.15	10.43	9.29	7.42
106k	9.25	11.43	9.09	6.96
120k	9.85	10.53	9.59	7.64
130k	9.55	11.33	9.69	7.37
150k	9.95	10.83	9.09	7.60
160k	9.35	10.93	9.19	7.44
173k	10.05	10.62	9.38	7.37
186k	9.33	10.81	9.07	7.79
200k	9.32	10.50	8.96	7.63

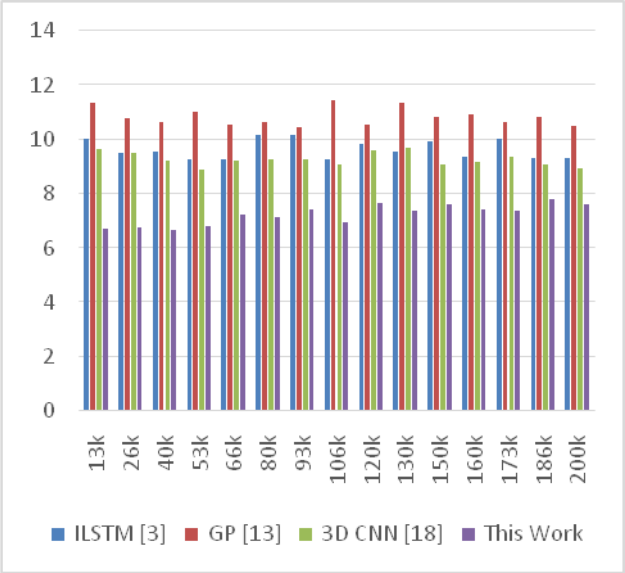

Figure 6. Delay Levels for different Yield Prediction Models under real-time multimodal scenarios

In terms of crop yield prediction delay performance levels, it can be seen from these results that the proposed model is 8.3% faster than ILSTM [3], 10.5% faster than GP [13], and 4.9% faster than 3D CNN [18]. This is because various deep learning models are being used to eliminate redundant features from samples that have been collected. Based on this analysis, it can be seen that the proposed model, when compared to various state-of-the-art models, is capable of high precision, better accuracy, higher recall, and faster performance, making it useful for a wide range of real-time crop yield prediction application scenarios.

V. CONCLUSION

Combining a multimodal feature analysis with a number of deep learning models, this work presents a novel method for crop yield prediction. The proposed model outperforms the current state-of-the-art models in terms of precision, accuracy, recall, AUC, and prediction delay.

The proposed model achieves precision gains of 12.5% when compared to ILSTM [3], 19.5% when compared to GP [13], and 18.3% when compared to 3D CNN [18]. This improvement is attributable to the utilization of multimodal feature analysis, which maximizes the feature variance across various sample types. The proposed method effectively captures and utilizes a variety of information by incorporating multiple deep learning models, thereby improving the precision of crop yield prediction.

In addition, the proposed model improves accuracy by 5.9%, 8.5%, and 3.4% relative to ILSTM [3, GP [13], and 3D CNN [18], respectively. This improvement is attributed to the combination of ResNet and Q Learning, which further improves feature variance maximization across various sample types. The application of these methods enables more accurate predictions of crop yield.

In comparison to ILSTM [3], GP [13], and 3D CNN [18], the proposed model improves recall by 14.5%, 23.5%, and 12.5%, respectively. This improvement is due to the implementation of multimodal feature processing, which includes geographic, spatial, temporal, and image analysis. Utilizing multiple deep learning models, the proposed method effectively captures the variability of features present in various image types, resulting in enhanced crop yield prediction recall performance.

In addition, the proposed model exhibits an AUC improvement of 14.5% relative to ILSTM [3], 19.4% relative to GP [13], and 18.8% relative to 3D CNN [18]. Several Q Learning, DDQN, and ResNet deep learning models are combined with multimodal feature analysis to achieve this improvement. This integration improves crop yield prediction AUC performance by maximizing feature variance across multiple sample types.

In addition to being 8.3% faster than ILSTM [3, 10.5% faster than GP [13, and 4.9% faster than 3D CNN [18], the proposed model demonstrates superior prediction delay performance. Using multiple deep learning models effectively reduces redundant features extracted from collected samples, thereby enhancing computational efficiency and accelerating prediction times.

Clearly, the proposed model outperforms cutting-edge models in terms of precision, accuracy, recall, AUC, and prediction delay, as demonstrated by the exhaustive analysis. Therefore, it can be utilized effectively in a variety of real-time crop yield prediction application scenarios. By integrating multimodal feature analysis with

multiple deep learning models, the model is able to efficiently capture and exploit the diversity of information, resulting in more accurate and effective predictions. This paper advances crop yield prediction research and creates new opportunities for enhancing agricultural productivity and decision-making process.

Future Scope

Based on the findings and outcomes of the study, a number of future research and development directions and areas can be identified for different use cases. The integration of additional data sources is also taking place. Although the proposed model employs multimodal feature analysis, it is possible to incorporate additional relevant data sources. Investigating the integration of additional data, such as information on weather patterns, soil quality, and pest infestations, may improve the accuracy of crop yield predictions. Incorporating data from cutting-edge technologies such as remote sensing and drones may also be investigated.

Modifying the hyper-parameters: The hyper-parameter settings have a substantial effect on the performance of deep learning models. Further study can improve the hyper-parameters of the proposed model, such as learning rates, regularization strategies, and network architectures. It may be possible to improve the accuracy of the predictions by optimizing these parameters.

Analyses of learning transfer: where pre-trained models are used as a starting point for a new task, can be studied in the context of crop yield prediction. Specific crop yield prediction datasets could be used to fine-tune pre-trained models on large-scale agricultural datasets or related tasks, potentially enhancing the performance of the model with less training time.

Extension to diverse agricultural and geographic regions: Although the proposed model focuses on crop yield prediction, it is applicable to a wide range of crops and geographic regions. Because each crop has distinct growth patterns and yield-influencing factors, a unique model could be trained and adjusted for each. Additionally, regional variations in soil, climate, and farming practices may necessitate a customized model for precise predictions in specific regions.

Implementation in real-world contexts: In order to evaluate the applicability and generalizability of the proposed model, it should be implemented and tested in actual agricultural contexts. The results of field tests and data collection from various farms and agricultural systems would provide valuable insight into the model's performance under varying conditions.

Estimating and integrating uncertainty: Estimating uncertainty is essential when making decisions regarding crop management. By investigating methods for estimating crop yield prediction uncertainty, the model's accuracy can be enhanced and farmers can be assisted in making more informed decisions. Methods such as ensemble methods and Bayesian deep learning could be researched for the purpose of quantifying uncertainty.

Using long-term data, crop yield prediction models should be validated to determine their robustness and dependability over extended time periods. It would be possible to perform a comprehensive evaluation of the proposed model's performance and its ability to recognize long-term trends and patterns if crop yield data from multiple seasons and years were available.

Creation of user-friendly interfaces: To facilitate the implementation of the proposed model, user-friendly interfaces and visualization tools can be developed. These user interfaces may present expected crop yields in an easy-to-understand format, allowing farmers and other decision-makers to comprehend and utilize the model's predictions.

Integration of technologies for precision agriculture: Farm management systems, Internet of Things (IoT) devices, and intelligent sensors are examples of the increasingly prevalent precision agriculture technologies. By integrating the crop yield prediction model with these technologies, real-time monitoring, decision support, and automation of agricultural operations would be possible. Exploring how precision agriculture and crop yield prediction can work together could result in significant improvements to farming techniques that are both efficient and sustainable for real-time scenarios.

The future scope of this paper includes developing user-friendly interfaces, integrating with precision agriculture technologies, extending the model to new crops and regions, incorporating uncertainty estimation, deploying the model in real-world settings, exploring transfer learning, fine-tuning hyper-parameters, and extending the model to new crops and regions. These areas for future research and development would further enhance the accuracy, applicability, and impact of the proposed crop yield prediction model process.

REFERENCES

[1] Y. Alebele et al., "Estimation of Crop Yield From Combined Optical and SAR Imagery Using Gaussian Kernel Regression," in IEEE Journal of Selected Topics in Applied Earth Observations and Remote Sensing, vol. 14, pp. 10520-10534, 2021, doi: 10.1109/JSTARS.2021.3118707.

[2] Y. Liu, Q. Yu, Q. Zhou, C. Wang, S. D. Bellingrath-Kimura and W. Wu, "Mapping the Complex Crop Rotation Systems in Southern China Considering Cropping Intensity, Crop Diversity, and Their Seasonal Dynamics," in IEEE Journal of Selected Topics in Applied Earth Observations and Remote Sensing, vol. 15, pp. 9584-9598, 2022, doi: 10.1109/JSTARS.2022.3218881.

[3] A. Mateo-Sanchis, J. E. Adsuara, M. Piles, J. Munoz-Marí, A. Perez-Suay and G. Camps-Valls, "Interpretable Long Short-Term Memory Networks for Crop Yield Estimation," in IEEE Geoscience and Remote Sensing Letters, vol. 20, pp. 1-5, 2023, Art no. 2501105, doi: 10.1109/LGRS.2023.3244064.

[4] D. Han et al., "Improving Wheat Yield Estimates by Integrating a Remotely Sensed Drought Monitoring Index Into the Simple Algorithm for Yield Estimate Model," in IEEE Journal of Selected Topics in Applied Earth Observations and Remote Sensing, vol. 14, pp. 10383-10394, 2021, doi: 10.1109/JSTARS.2021.3119398.

[5] D. Han et al., "Improving Wheat Yield Estimates by Integrating a Remotely Sensed Drought Monitoring Index Into the Simple Algorithm for Yield Estimate Model," in IEEE Journal of Selected Topics in Applied Earth Observations and Remote Sensing, vol. 14, pp. 10383-10394, 2021, doi: 10.1109/JSTARS.2021.3119398.

[6] S. Wu, J. Ren, Z. Chen, P. Yang, H. Li and J. Liu, "Evaluation of Winter Wheat Yield Simulation Based on Assimilating LAI Retrieved From Networked Optical and SAR Remotely Sensed Images Into the WOFOST Model," in IEEE Transactions on Geoscience and Remote Sensing, vol. 59, no. 11, pp. 9071-9085, Nov. 2021, doi: 10.1109/TGRS.2020.3038205.

[7] H. Huang et al., "The Improved Winter Wheat Yield Estimation by Assimilating GLASS LAI Into a Crop Growth Model With the Proposed Bayesian Posterior-Based Ensemble Kalman Filter," in IEEE Transactions on Geoscience and Remote Sensing, vol. 61, pp. 1-18, 2023, Art no. 4401818, doi: 10.1109/TGRS.2023.3259742.

[8] F. Ji, J. Meng, Z. Cheng, H. Fang and Y. Wang, "Crop Yield Estimation at Field Scales by Assimilating Time Series of Sentinel-2 Data Into a Modified CASA-WOFOST Coupled Model," in IEEE Transactions on Geoscience and Remote Sensing, vol. 60, pp. 1-14, 2022, Art no. 4400914, doi: 10.1109/TGRS.2020.3047102.

[9] Z. Ramzan, H. M. S. Asif, I. Yousuf and M. Shahbaz, "A Multimodal Data Fusion and Deep Neural Networks Based Technique for Tea Yield Estimation in Pakistan Using Satellite Imagery," in IEEE Access, vol. 11, pp. 42578-42594, 2023, doi: 10.1109/ACCESS.2023.3271410.

[10] A. Reyana, S. Kautish, P. M. S. Karthik, I. A. Al-Baltah, M. B. Jasser and A. W. Mohamed, "Accelerating Crop Yield: Multisensor Data Fusion and Machine Learning for Agriculture Text Classification," in IEEE Access, vol. 11, pp. 20795-20805, 2023, doi: 10.1109/ACCESS.2023.3249205.

[11] S. Yang et al., "Integration of Crop Growth Model and Random Forest for Winter Wheat Yield Estimation From UAV Hyperspectral Imagery," in IEEE Journal of Selected Topics in Applied Earth Observations and Remote Sensing, vol. 14, pp. 6253-6269, 2021, doi: 10.1109/JSTARS.2021.3089203.

[12] Z. Yang, C. Diao and F. Gao, "Towards Scalable Within-Season Crop Mapping With Phenology Normalization and Deep Learning," in IEEE Journal of Selected Topics in Applied Earth Observations and Remote Sensing, vol. 16, pp. 1390-1402, 2023, doi: 10.1109/JSTARS.2023.3237500.

[13] L. Martínez-Ferrer, M. Piles and G. Camps-Valls, "Crop Yield Estimation and Interpretability With Gaussian Processes," in IEEE Geoscience and Remote Sensing Letters, vol. 18, no. 12, pp. 2043-2047, Dec. 2021, doi: 10.1109/LGRS.2020.3016140.

[14] Y. Ma, Z. Yang and Z. Zhang, "Multisource Maximum Predictor Discrepancy for Unsupervised Domain Adaptation on Corn Yield Prediction," in IEEE Transactions on Geoscience and Remote Sensing, vol. 61, pp. 1-15, 2023, Art no. 4401315, doi: 10.1109/TGRS.2023.3247343.

[15] A. F. Haufler, J. H. Booske and S. C. Hagness, "Microwave Sensing for Estimating Cranberry Crop Yield: A Pilot Study Using Simulated Canopies and Field Measurement Testbeds," in IEEE Transactions on Geoscience and Remote Sensing, vol. 60, pp. 1-11, 2022, Art no. 4400411, doi: 10.1109/TGRS.2021.3050171.

[16] M. Qiao et al., "Exploiting Hierarchical Features for Crop Yield Prediction Based on 3-D Convolutional Neural Networks and Multikernel Gaussian Process," in IEEE Journal of Selected Topics in Applied Earth Observations and Remote Sensing, vol. 14, pp. 4476-4489, 2021, doi: 10.1109/JSTARS.2021.3073149.

[17] M. Qiao et al., "Exploiting Hierarchical Features for Crop Yield Prediction Based on 3-D Convolutional Neural Networks and Multikernel Gaussian Process," in IEEE Journal of Selected Topics in Applied Earth Observations and Remote Sensing, vol. 14, pp. 4476-4489, 2021, doi: 10.1109/JSTARS.2021.3073149.

[18] B. Yang, J. Guo, J. Liu and X. Ye, "PPCE: A Practical Loss for Crop Mapping Using Phenological Prior," in IEEE Geoscience and Remote Sensing Letters, vol. 20, pp. 1-5, 2023, Art no. 5000605, doi: 10.1109/LGRS.2022.3230421.

[19] E. Myers, J. Kerekes, C. Daughtry and A. Russ, "Effects of Satellite Revisit Rate and Time-Series Smoothing Method on Throughout-Season Maize Yield Correlation Accuracy," in IEEE Journal of Selected Topics in Applied Earth Observations and Remote Sensing, vol. 14, pp. 12007-12021, 2021, doi: 10.1109/JSTARS.2021.3129148.

[20] N. Farmonov et al., "Crop Type Classification by DESIS Hyperspectral Imagery and Machine Learning Algorithms," in IEEE Journal of Selected Topics in Applied Earth Observations and Remote Sensing, vol. 16, pp. 1576-1588, 2023, doi: 10.1109/JSTARS.2023.3239756.

[21] S. M. M. Nejad, D. Abbasi-Moghadam, A. Sharifi, N. Farmonov, K. Amankulova and M. László, "Multispectral Crop Yield Prediction Using 3D-Convolutional Neural Networks and Attention Convolutional LSTM Approaches," in IEEE Journal of Selected Topics in Applied Earth Observations and Remote Sensing, vol. 16, pp. 254-266, 2023, doi: 10.1109/JSTARS.2022.3223423.

[22] C. Silva-Perez, A. Marino and I. Cameron, "Learning-Based Tracking of Crop Biophysical Variables and Key Dates Estimation From Fusion of SAR and Optical Data," in IEEE Journal of Selected Topics in Applied Earth Observations and Remote Sensing, vol. 15, pp. 7444-7457, 2022, doi: 10.1109/JSTARS.2022.3203248.

[23] M. R. Khokher et al., "Early Yield Estimation in Viticulture Based on Grapevine Inflorescence Detection and Counting in Videos," in IEEE Access, vol. 11, pp. 37790-37808, 2023, doi: 10.1109/ACCESS.2023.3263238.

[24] M. H. Riaz, H. Imran, H. Alam, M. A. Alam and N. Z. Butt, "Crop-Specific Optimization of Bifacial PV Arrays for Agrivoltaic Food-Energy Production: The Light-Productivity-Factor Approach," in IEEE Journal of Photovoltaics, vol. 12, no. 2, pp. 572-580, March 2022, doi: 10.1109/JPHOTOV.2021.3136158.

[25] H. C. Verma et al., "Development of LR-PCA Based Fusion Approach to Detect the Changes in Mango Fruit Crop by Using Landsat 8 OLI Images," in IEEE Access, vol. 10, pp. 85764-85776, 2022, doi: 10.1109/ACCESS.2022.3194000.

[26] Y. Ma and Z. Zhang, "A Bayesian Domain Adversarial Neural Network for Corn Yield Prediction," in IEEE Geoscience and Remote Sensing Letters, vol. 19, pp. 1-5, 2022, Art no. 5513705, doi: 10.1109/LGRS.2022.3211444.

[27] Y. Yan et al., "Integration of Canopy Water Removal and Spectral Triangle Index for Improved Estimations of Leaf Nitrogen and Grain Protein Concentrations in Winter Wheat," in IEEE Transactions on Geoscience and Remote Sensing, vol. 61, pp. 1-18, 2023, Art no. 4404118, doi: 10.1109/TGRS.2023.3277456.

[28] A. K. Dwivedi, A. K. Singh, D. Singh and H. Kumar, "Development of an Adaptive Linear Mixture Model for Decomposition of Mixed Pixels to Improve Crop Area Estimation Using Artificial Neural Network," in IEEE Access, vol. 11, pp. 5714-5723, 2023, doi: 10.1109/ACCESS.2023.3236665.

[29] N. Rasheed, S. A. Khan, A. Hassan and S. Safdar, "A Decision Support Framework for National Crop Production Planning," in IEEE Access, vol. 9, pp. 133402-133415, 2021, doi: 10.1109/ACCESS.2021.3115801.

[30] N. Ullah, J. A. Khan, L. A. Alharbi, A. Raza, W. Khan and I. Ahmad, "An Efficient Approach for Crops Pests Recognition and Classification Based on Novel DeepPestNet Deep Learning Model," in IEEE Access, vol. 10, pp. 73019-73032, 2022, doi: 10.1109/ACCESS.2022.3189676.

[31] X. Li, Y. Dong, Y. Zhu and W. Huang, "Enhanced Leaf Area Index Estimation With CROP-DualGAN Network," in IEEE Transactions on Geoscience and Remote Sensing, vol. 61, pp. 1-10, 2023, Art no. 5514610, doi: 10.1109/TGRS.2022.3230354.

[32] N. Romero-Puig, J. M. Lopez-Sanchez and M. Busquier, "Evaluation of PolInSAR Observables for Crop-Type Mapping Using Bistatic TanDEM-X Data," in IEEE Geoscience and Remote Sensing Letters, vol. 19, pp. 1-5, 2022, Art no. 4508005, doi: 10.1109/LGRS.2022.3175689.

[33] W. Wang et al., "AAVI: A Novel Approach to Estimating Leaf Nitrogen Concentration in Rice From Unmanned Aerial Vehicle Multispectral Imagery at Early and Middle Growth Stages," in IEEE Journal of Selected Topics in Applied Earth Observations and Remote Sensing, vol. 14, pp. 6716-6728, 2021, doi: 10.1109/JSTARS.2021.3086580.

[34] S. I. Moazzam et al., "A Patch-Image Based Classification Approach for Detection of Weeds in Sugar Beet Crop," in IEEE Access, vol. 9, pp. 121698-121715, 2021, doi: 10.1109/ACCESS.2021.3109015.

[35] M. D. Maas, M. Salvia, P. C. Spennemann and M. E. Fernandez-Long, "Robust Multisensor Prediction of Drought-Induced Yield Anomalies of Soybeans in Argentina," in IEEE Geoscience and Remote Sensing Letters, vol. 19, pp. 1-4, 2022, Art no. 2504804, doi: 10.1109/LGRS.2022.3171415.

[36] X. Qu et al., "Monitoring Lodging Extents of Maize Crop Using Multitemporal GF-1 Images," in IEEE Journal of Selected Topics in Applied Earth Observations and Remote Sensing, vol. 15, pp. 3800-3814, 2022, doi: 10.1109/JSTARS.2022.3170345.

[37] R. Priya, D. Ramesh and V. Udutalapally, "NSGA-2 Optimized Fuzzy Inference System for Crop Plantation Correctness Index Identification," in IEEE Transactions on Sustainable Computing, vol. 7, no. 1, pp. 172-188, 1 Jan.-March 2022, doi: 10.1109/TSUSC.2021.3064417.

[38] C. Hu, S. Xie, D. Song, J. A. Thomasson, R. G. H. IV and M. Bagavathiannan, "Algorithm and System Development for Robotic Micro-Volume Herbicide Spray Towards Precision Weed Management," in IEEE Robotics and Automation Letters, vol. 7, no. 4, pp. 11633-11640, Oct. 2022, doi: 10.1109/LRA.2022.3191240.

[39] Y. Du, J. Jiang, Z. Liu and Y. Pan, "Combining a Crop Growth Model With CNN for Underground Natural Gas Leakage Detection Using Hyperspectral Imagery," in IEEE Journal of Selected Topics in Applied Earth Observations and Remote Sensing, vol. 15, pp. 1846-1856, 2022, doi: 10.1109/JSTARS.2022.3150089.

[40] I. Aneece, D. Foley, P. Thenkabail, A. Oliphant and P. Teluguntla, "New Generation Hyperspectral Data From DESIS Compared to High Spatial Resolution Planet Scope Data for Crop Type Classification," in IEEE Journal of Selected Topics in Applied Earth Observations and Remote Sensing, vol. 15, pp. 7846-7858, 2022, doi: 10.1109/JSTARS.2022.3204223.

[41] Y. Zhang et al., "Enhanced Feature Extraction From Assimilated VTCI and LAI With a Particle Filter for Wheat Yield Estimation Using Cross-Wavelet Transform," in IEEE Journal of Selected Topics in Applied Earth Observations and Remote Sensing, vol. 16, pp. 5115-5127, 2023, doi: 10.1109/JSTARS.2023.3283240.

[42] P. Singh et al., "Biospeckle-Based Sensor for Characterization of Charcoal Rot (Macrophomina Phaseolina (Tassi) Goid) Disease in Soybean (Glycine Max (L.) Merr.) Crop," in IEEE Access, vol. 9, pp. 31562-31574, 2021, doi: 10.1109/ACCESS.2021.3059868.

[43] U. Shafi et al., "Embedded AI for Wheat Yellow Rust Infection Type Classification," in IEEE Access, vol. 11, pp. 23726-23738, 2023, doi: 10.1109/ACCESS.2023.3254430.

[44] J. Jiang et al., "MACA: A Relative Radiometric Correction Method for Multiflight Unmanned Aerial Vehicle Images Based on Concurrent Satellite Imagery," in IEEE Transactions on Geoscience and Remote Sensing, vol. 60, pp. 1-14, 2022, Art no. 5408314, doi: 10.1109/TGRS.2022.3158644.

[45] J. Jiang et al., "MACA: A Relative Radiometric Correction Method for Multiflight Unmanned Aerial Vehicle Images Based on Concurrent Satellite Imagery," in IEEE Transactions on Geoscience and Remote Sensing, vol. 60, pp. 1-14, 2022, Art no. 5408314, doi: 10.1109/TGRS.2022.3158644.

[46] S. Das, A. Biswas, V. C and P. Sinha, "Deep Learning Analysis of Rice Blast Disease Using Remote Sensing Images," in IEEE Geoscience and Remote Sensing Letters, vol. 20, pp. 1-5, 2023, Art no. 2500905, doi: 10.1109/LGRS.2023.3244324.

[47] D. Yuan, S. Zhang, H. Li, J. Zhang, S. Yang and Y. Bai, "Improving the Gross Primary Productivity Estimate by Simulating the Maximum Carboxylation Rate of the Crop Using Machine Learning Algorithms," in IEEE Transactions on Geoscience and Remote Sensing, vol. 60, pp. 1-15, 2022, Art no. 4413115, doi: 10.1109/TGRS.2022.3200988.

[48] H. R. Bukhari et al., "Assessing the Impact of Segmentation on Wheat Stripe Rust Disease Classification Using Computer Vision and Deep Learning," in IEEE Access, vol. 9, pp. 164986-165004, 2021, doi: 10.1109/ACCESS.2021.3134196.

[49] S. Shorewala, A. Ashfaque, R. Sidharth and U. Verma, "Weed Density and Distribution Estimation for Precision Agriculture Using Semi-Supervised Learning," in IEEE Access, vol. 9, pp. 27971-27986, 2021, doi: 10.1109/ACCESS.2021.3057912.

[50] H. R. Seireg, Y. M. K. Omar, F. E. A. El-Samie, A. S. El-Fishawy and A. Elmahalawy, "Ensemble Machine Learning Techniques Using Computer Simulation Data for Wild Blueberry Yield Prediction," in IEEE Access, vol. 10, pp. 64671-64687, 2022, doi: 10.1109/ACCESS.2022.3181970.

[51] S. A. Lohi and C. Bhatt, "Design of a Crop Disease Detection Model using Multi-parametric Bio-inspired Feature Representation and Ensemble Classification," 2023 4th International Conference on Innovative Trends in Information Technology (ICITIIT), Kottayam, India, 2023, pp. 1-6, doi: 10.1109/ICITIIT57246.2023.10068649.

[52] Lohi, Snehal A., Bhatt, C. Empirical Analysis of Crop Yield Prediction and Disease Detection Systems: A Statistical Perspective. In: Tuba, M., Akashe, S., Joshi, A. (eds) ICT Infrastructure and Computing. Lecture Notes in Networks and Systems, vol 520. Springer, Singapore. https://doi.org/10.1007/978-981-19-5331-6_6.

[53] Snehal A. Lohi-Bode, et.al. (2023) Integrating Two-Level Reinforcement Learning Process for Enhancing Task Scheduling Efficiency in a Complex Problem-Solving Environment, Taylor & Francis IETE Journal of Research https://DOI: 10.1080/03772063.2023.2185298.

[54] Snehal A. Lohi-Bode, C. Bhatt (2023) “Creation of Harvest Productivity Projection Method (HPPM) Using Machine Learning Framework through Combating Infection and Generating Knowledge”, in ISTE Journal (UGC CARE).

[55] Snehal Lohi-Bode et. al., (2023) Integrating Two-Level Reinforcement Learning Process for Enhancing Task Scheduling Efficiency in a Complex Problem-Solving Environment, IETE Journal of Research, DOI: 10.1080/03772063.2023.2185298.

[56] R. Jogekar and N. Tiwari, "Summary of Leaf-based plant disease detection systems: A compilation of study findings to classify the leaf disease classification schemes," 2020 Fourth World Conference on Smart Trends in Systems, Security and Sustainability (WorldS4), London, UK, 2020, pp. 745-750, 10.1109/WorldS450073.2020.9210401

[57] Lohi, S.A., Tiwari, N. (2021). Assessment of Suitability of Metaheuristics and Machine Learning for Task Scheduling Process: A Review of Aptness in Heavy Task Environments. In: Zhang, YD., Senjyu, T., SO–IN, C., Joshi, A. (eds) Smart Trends in Computing and Communications: Proceedings of SmartCom 2020. Smart Innovation, Systems and Technologies, vol 182. Springer, Singapore. https://doi.org/10.1007/978-981-15-5224-3_41.

[58] Lohi Shantanu, et. al., “Assessment of suitability of metaheuristics and machine learning for task scheduling process: A review of aptness in heavy task environments”, Smart Trends in Computing and Communications: Proceedings of SmartCom 2020, Advances in Intelligent Systems and Computing, vol. 182. Springer, Singapore, (2020).

[59] Lohi Shantanu, et.al., “An Exceedingly efficient, enhanced and cost-effective task scheduling algorithm for complex layered factual systems” International Journal of Future Generation and Communication Networks, Vol. 13, Issue 3, 2020, pp. 3527-3536.

[60] Lohi S.A. et. al., (2019), “Analytical Assessment of Nature-Inspired Metaheuristic Algorithms to Elucidate Assembly Line Task Scheduling Problem”, Information and Communication Technology for Sustainable Development. Advances in Intelligent Systems and Computing, vol. 933. Springer, Singapore, (2020).

[61] Harish Gorewar, N Tiwari "Inferring optimal electoral roll creation, verification and management strategies: System development reviews", 2020 Fourth World Conference on Smart Trends in Systems, Security and Sustainability (WorldS4), London, UK, 2020, pp. 751-756, 10.1109/WorldS450073.2020.9210401